NeuroImage 200 (2019) 601–606

Contents lists available at ScienceDirect

NeuroImage

journal homepage: www.elsevier.com/locate/neuroimage

QUEST MRI assessment of fetal brain oxidative stress *in utero*

Bruce A. Berkowitz [a,*], Roberto Romero [b,c,d,e,f], Robert H. Podolsky [g], Karen M. Lins-Childers [g], Yimin Shen [h], Tilman Rosales [a], Youssef Zaim Wadghiri [i], D. Minh Hoang [i], Marcia Arenas-Hernandez [b,j], Valeria Garcia-Flores [b,j], George Schwenkel [b,j], Bogdan Panaitescu [b,j], Nardhy Gomez-Lopez [b,j,k,**]

[a] *Department of Ophthalmology, Visual and Anatomical Sciences, Wayne State University School of Medicine, Detroit, Michigan, 48201, USA*
[b] *Perinatology Research Branch, Division of Obstetrics and Maternal-Fetal Medicine, Division of Intramural Research, Eunice Kennedy Shriver National Institute of Child Health and Human Development, National Institutes of Health, U.S. Department of Health and Human Services (NICHD/NIH/DHHS), Bethesda, Maryland, 20847, and Detroit, Michigan, 48201, USA*
[c] *Department of Obstetrics and Gynecology, University of Michigan Health System, Ann Arbor, Michigan, 48109, USA*
[d] *Department of Epidemiology and Biostatistics, College of Human Medicine, Michigan State University, East Lansing, Michigan, 48824, USA*
[e] *Center for Molecular Medicine and Genetics, Wayne State University, Detroit, Michigan, 48201, USA*
[f] *Detroit Medical Center, Detroit, Michigan, 48201, USA*
[g] *Beaumont Research Institute, Beaumont Health, Royal Oak, Michigan, 48073, USA*
[h] *Department of Radiology, Wayne State University School of Medicine, Detroit, Michigan, 48201, USA*
[i] *Department of Radiology, Center for Advanced Imaging Innovation and Research (CAI2R), Bernard and Irene Schwartz Center for Biomedical Imaging, NYU School of Medicine and NYU Langone Health, New York, New York, 10016, USA*
[j] *Department of Obstetrics and Gynecology, Wayne State University School of Medicine, Detroit, Michigan, 48201, USA*
[k] *Department of Biochemistry, Microbiology and Immunology, Wayne State University School of Medicine, Detroit, Michigan, 48201, USA*

ARTICLE INFO

Keywords:
Quench-assisted MRI
Free radicals
Reactive oxygen species
Embryo

ABSTRACT

Purpose: To achieve sufficient precision of R1 (=1/T1) maps of the fetal brain *in utero* to perform QUEnch-assiSTed (QUEST) MRI in which a significant anti-oxidant-induced reduction in R1 indicates oxidative stress.
Methods: C57BL/6 mouse fetuses *in utero* were gently and non-surgically isolated and secured using a homemade 3D printed clip. Using a commercial receive-only surface coil, brain maps of R1, an index sensitive to excessive and continuous free radical production, were collected using either a conventional Cartesian or a non-Cartesian (periodically rotated overlapping parallel lines with enhanced reconstruction) progressive saturation sequence. Data were normalized to the shortest TR time to remove bias. To assess oxidative stress, brain R1 maps were acquired on the lipopolysaccharide (LPS) model of preterm birth ± rosiglitazone (ROSI, which has anti-oxidant properties); phosphate buffered saline (PBS) controls ± ROSI were similarly studied.
Results: Sufficient quality R1 maps were generated by a combination of the 3D printed clip, surface coil detection, non-Cartesian sequence, and normalization scheme ensuring minimal fetal movement, good detection sensitivity, reduced motion artifacts, and minimal baseline variations, respectively. In the LPS group, the combined caudate-putamen and thalamus region R1 was reduced ($p < 0.05$) with ROSI treatment consistent with brain oxidative stress; no evidence for oxidative stress was found in the pons region. In the PBS control group, brain R1's did not change with ROSI treatment.
Conclusion: The sensitivity and reproducibility of the combined approaches described herein enabled first-time demonstration of regional oxidative stress measurements of the fetal brain *in utero* using QUEST MRI.

* Corresponding author. Wayne State University School of Medicine, 540 E. Canfield, Detroit, MI, 48201, USA.
** Corresponding author. Department of Obstetrics and Gynecology, Wayne State University School of Medicine, Perinatology Research Branch, NICHD/NIH/DHHS, 275 E. Hancock, Detroit, MI, 48201, USA.
E-mail addresses: baberko@med.wayne.edu (B.A. Berkowitz), nardhy.gomez-lopez@wayne.edu (N. Gomez-Lopez).

https://doi.org/10.1016/j.neuroimage.2019.05.069
Received 9 March 2019; Received in revised form 15 May 2019; Accepted 27 May 2019
Available online 31 May 2019

1. Introduction

Intra-amniotic infection/inflammation has been implicated as a major risk factor for fetal brain injury, preterm labor and delivery, poor postnatal neurological outcomes, and greater mortality (Romero et al., 2014). While the underlying mechanisms remain unclear, experimental studies using cells and excised tissue have suggested that fetal brain oxidative stress contributes to lipopolysaccharide (LPS)-induced fetal loss and abnormal fetal brain development (Chao et al., 2016). Thus, early detection of fetal brain oxidative stress *in utero* may be useful for personalizing anti-oxidant treatment to mitigate fetal inflammatory response syndrome and its adverse downstream consequences (Gomez et al., 1998; Gotsch et al., 2007; Ginsberg et al., 2017). However, conventional methods for measuring oxidative damage in fetal brains are limited to *ex vivo* studies of excised tissue, and thus cannot be performed *in vivo*.

To address this need, we investigated a new method of QUEnch-assiSTed (QUEST) MRI that measures excessive free radical production *in vivo* without a contrast agent (Berkowitz, 2018). In this experiment, continuous and asynchronous production of paramagnetic free radicals can increase R1 (=1/T1) as revealed by a reduction in R1 after administration of anti-oxidants (i.e., a quench) (Berkowitz, 2018). Neuronal QUEST MRI studies have been validated against "gold standard" free radical assay *ex vivo* in several animal models (Berkowitz, 2018). However, it remains a substantial challenge to obtain reproducible R1 values in the fetal brain *in utero* given the respiratory and heart movements of the dam and spontaneous movements of the fetus in its amniotic sac (Zhang et al., 2018).

In this study, we combine four strategies to achieve the goal of performing QUEST MRI in the fetal brain *in utero*. First, we utilize a 3D printed clip to gently secure individual fetuses *in situ* to stabilize spontaneous movements. We then compare progressive saturation recovery R1 data collected using either a standard Cartesian (i.e., spin-echo) or a non-Cartesian (periodically rotated overlapping parallel lines with enhanced reconstruction) sequence to determine which best minimized motion artifacts without respiratory gating. Third, we used surface coil reception to maximize the filling factor resulting in the improvement of the signal-to-noise ratio over a whole-body coil. Finally, the R1 data set was normalized to the shortest repetition time (TR) to reduce coil inhomogeneities and slice bias for a more precise R1 estimate. The usefulness of the combined approaches for detecting localized brain oxidative stress with QUEST MRI was then tested in a lipopolysaccharide (LPS) mouse model of preterm labor (Gomez-Lopez et al., 2018). Rosiglitazone (ROSI) was used in the LPS model because of its anti-oxidant/anti-inflammatory properties and because it mitigates preterm birth (St Louis et al., 2016; Xu et al., 2016; Gomez-Lopez et al., 2017; Kadam et al., 2017).

2. Methods

All procedures were approved by the Institutional Animal Care and Use Committee (IACUC) at Wayne State University (Protocols No. A 07-03-15 & 18-03-0584).

2.1. Mice

C57BL/6 mice were purchased from The Jackson Laboratory in Bar Harbor, ME, USA, and bred in the animal care facility at the C.S. Mott Center for Human Growth and Development at Wayne State University, Detroit, MI, USA. All mice were kept under a circadian cycle (light:-dark = 12:12 h). Females, 8–12 weeks old, were bred with males of proven fertility. Female mice were checked daily in the morning for the appearance of a vaginal plug, which indicated 0.5 days post coitum (dpc). Females were then housed separately from the males, their weights were monitored daily, and a gain of two or more grams by 12.5 dpc confirmed pregnancy.

2.2. Animal model of preterm birth induced by intra-amniotic inflammation

Intra-amniotic administration of LPS (Gomez-Lopez et al., 2018) (Fig. 1): Pregnant B6 mice were anesthetized on 16.5 dpc (or embryonic day/E) by inhalation of 2–3% isoflurane (Aerrane, Baxter Healthcare Corporation, Deerfield, IL, USA) and 1–2 L/min of oxygen in an induction chamber. Anesthesia was maintained with a mixture of 1.5–2% isoflurane and 1.5–2 L/min of oxygen. Mice were positioned on a heating pad and stabilized with adhesive tape (Fig. 1). Fur removal from the abdomen and thorax was achieved by applying Nair cream (Church & Dwight Co., Inc., Ewing, NJ, USA) to those areas. Body temperature was maintained in the range of 37 ± 1 °C and detected with a rectal probe (VisualSonics, Toronto, Ontario, Canada), and respiratory and heart rates were monitored by electrodes embedded in the heating pad. An ultrasound probe included in the Vevo 2100 Imaging System (VisualSonics, Toronto, Ontario, Canada) was fixed and mobilized with a mechanical holder, and the transducer was slowly moved toward the abdomen. Ultrasound-guided intra-amniotic injection of LPS (*Escherichia coli* O111:B4; Sigma-Aldrich, St. Louis, MO, USA) at a concentration of

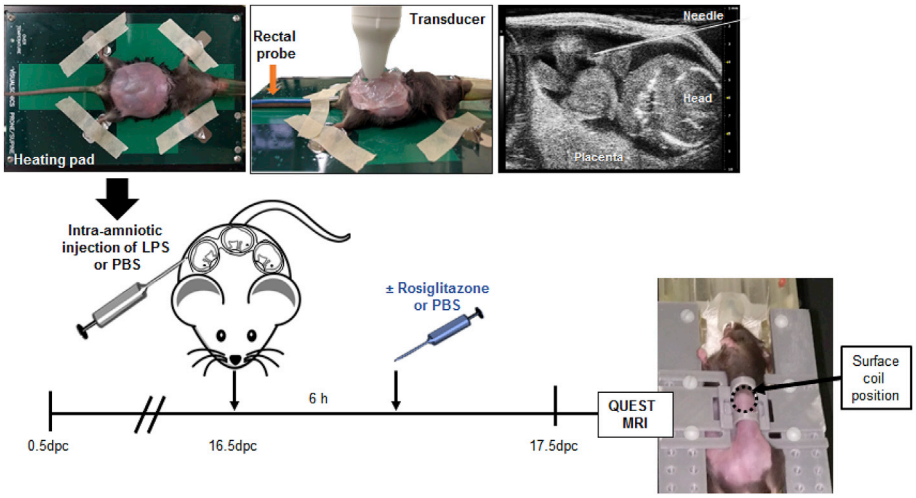

Fig. 1. *Top row.* Experimental design. Dams (E16.5) were anesthetized and underwent an ultrasound procedure. *Bottom row:* Timeline for intra-amniotic injection followed by treatment with ROSI or saline, prior to QUEST MRI. dpc, days post coitum, and photograph illustrating the position of the 3D printed clip and surface coil position (dotted line circle).

100 ng dissolved in 25 μL of sterile 1X phosphate-buffered saline (PBS; Fisher Scientific Bioreagents, Fair Lawn, NJ, USA) was performed in each amniotic sac using a 30-gauge needle (BD PrecisionGlide Needle, Becton Dickinson, Franklin Lakes, NJ, USA). Controls were injected with 25 μL of sterile 1X PBS. The syringe was stabilized by a mechanical holder (VisualSonics, Toronto, Ontario, Canada). Following ultrasound, mice were placed under a heat lamp for recovery (defined as when the mouse resumes normal activity, such as walking and responding), which typically occurs 10–20 min after removal from anesthesia.

2.3. Treatment with ROSI

Six hours following the intra-amniotic injection with LPS, pregnant mice were intraperitoneally injected with 10 mg/kg of ROSI (Selleckchem, Houston, TX, USA). Control pregnant mice were injected with PBS and ROSI. MRI was performed 9–10 h after injection with ROSI (Fig. 1).

2.4. QUEST MRI

Before MRI examination, dams were anesthetized with isoflurane (1.25% with 1 L/min Medical air). A set of 3D printed clips were designed in-house using Solidworks software (Dassault Systems, www.solidworks.com) with the goal of gently immobilizing the fetus of interest *in utero* without altering its physiology. The 3D printed version of the clip was fabricated with Acrylonitrile Butadiene Styrene (ABS) using a Makerbot replicator Z18 (Makerbot Industries, Brooklyn, NY, USA). The fabricated clip secured the fetus by gripping on the skin side up before placing the surface coil (Fig. 1). This setup was designed to restrain the movements of the fetus during imaging while ensuring patent blood flow between the dam and the fetus throughout the examination. To check for effects of the clip on the blood flow of the restrained fetus, a preliminary experiment was performed using a stage mimicking the MRI experimental conditions. The blood flow of the whole clipped fetus was assessed using Doppler ultrasound and did not show any detrimental effect during a 2-h window of examination (data not shown).

High resolution R1 data were acquired on a 7T system (Bruker ClinScan, Billerica, MA, USA) using a commercial receive-only surface coil (1.0 cm diameter) that was part of the coil set for the Clinscan. In all cases, several single spin-echo (time to echo [TE] 13 ms, $7 \times 7\ mm^2$, matrix size 160×320, slice thickness 600 μm, in-plane resolution 21.875 μm) images were acquired using either a conventional spin-echo sequence or a periodically rotated overlapping parallel lines with enhanced reconstruction (called BLADE on the Clinscan system) acquisition. In both experiments, different TRs were used in the following order (number of scans per TR in parentheses): TR 0.15 s (6), 3.50 s (1), 1.00 s (2), 1.90 s (1), 0.35 s (4), 2.70 s (1), 0.25 s (5), and 0.50 s (3). Periodically rotated overlapping parallel lines with enhanced reconstruction motion reduction sequences are designed to minimize motion by sampling k-space at different small angles using a set of multiple parallel phase-encoded lines (Pipe, 1999). To compensate for reduced signal-noise ratios at shorter TRs, progressively more images were collected for averaging as the TR decreased. The slice chosen for these studies is shown in Fig. 2 using a high-resolution MRI histology image shared by Dr. G. Allan Johnson (http://www.civm.duhs.duke.edu/index.htm) (Petiet et al., 2008). The three brain regions of interest (ROI) within the slice in Fig. 2 were chosen because they could be reliably identified on all fetal brain images.

2.5. MRI data analysis

Within each R1 data set of 23 images, images acquired with the same TR were first registered (rigid body) and then averaged to generate a stack of 8 images. These averaged images were then registered across average images. It is well known that using imperfect slice profiles leads to systematically underestimated R1 values [Chapter 18 in (Haacke et al., 1999)]. To correct for this bias, we normalized to the shorter TR which results in a more accurate R1 estimate (Dr. E.M. Haacke, personal communication). The normalization procedure was to first apply a 3×3 Gaussian smoothing filter (performed three times) on only the image set acquired at TR 150 ms to minimize noise and emphasize signal, and to act as a low pass filter to infer the B1 map and account for RF coil in homogeneities. The smoothed TR 150 ms image was then divided into the rest of the images of that R1 data set. Preliminary experiments (not shown) found that this procedure substantially minimized the day-to-day variation in the R1 profile previously noted and obviated the need for a "vanilla control" group used previously to correct for day-to-day variations (Berkowitz et al., 2015; Berkowitz et al., 2016). R1 maps were calculated using the 7 normalized images via fitting to a three-parameter T1 equation ($y = a + b*(\exp(-c*TR))$, where a, b, and c are fitted parameters) on a pixel-by-pixel basis using in-house R scripts.

2.6. Statistical analysis

Data are presented as mean ± standard error of the mean (SEM), and a significance level of 0.05 was used for all analyses except as noted below. R1 was analyzed differently for the combined caudate-putamen and thalamus ROI (hemisphere) and the pons ROI given that the hemisphere ROI was measured on both the left and right sides. For the pons ROI, we used analysis of variance to examine the differences among the groups.

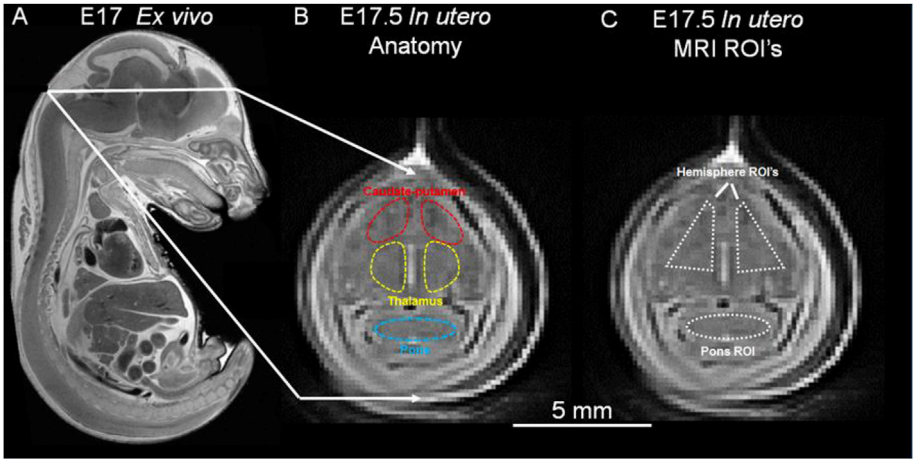

Fig. 2. A) A high resolution MRI histology image illustrates the position of the slice in this study (Petiet et al., 2008). Brain regions evaluated: caudate putamen [red dotted region in B)] and thalamus [yellow dotted region in B)] in the hemisphere ROI in C), and pons [blue dotted region in B)] in the pons ROI in C).

The overall test for differences in the pons ROI among the groups was not statistically significant ($p = 0.25$), so no further analyses were done. For the hemisphere ROI, we used a mixed linear model that included the treatment group as a fixed effect and a random intercept for mouse. The overall test for differences among the groups was statistically significant ($p = 0.0004$), leading us to examine the differences among the groups by using contrasts and the mixed linear model. We first examined the interaction between ROSI and LPS, using a significance level of 0.1, as the power is often much lower for interactions. The interaction of ROSI and LPS was significant at this level ($p = 0.06$), leading us to examine the effect of ROSI within the PBS and LPS groups separately. All analyses were conducted in SAS 9.4, using Proc Mixed. The contrasts were constructed using "Estimate" statements in Proc Mixed and the resulting standard error and degrees of freedom were calculated using the Kenward-Roger method.

3. Results

3.1. 3D printed clip and surface coil reception

Initial studies of the fetal brain *in utero* involved a 3D printed clip to stabilize fetal movement and optimize the surface coil filling factor. These two design elements allowed for the collection of interpretable T2 images. However, as shown in Fig. 3, no discernible brain structure was observed using conventional spin echo acquisition, likely due to maternal breathing-induced motion artifacts, thus, preventing the collection of reliable R1 information (Fig. 3 A).

3.2. BLADE acquisition

Compared to standard Cartesian acquisition (Fig. 3 A), the BLADE sequence minimized the contribution of motion artifacts and (together with the 3D printed clip) yielded sufficient T1 anatomical images and R1 maps (Fig. 3 B) that were reproducible over a 30-min period (Fig. 3 C). The usefulness of this approach is also illustrated by representative images from each of the four groups (Fig. 4, top row).

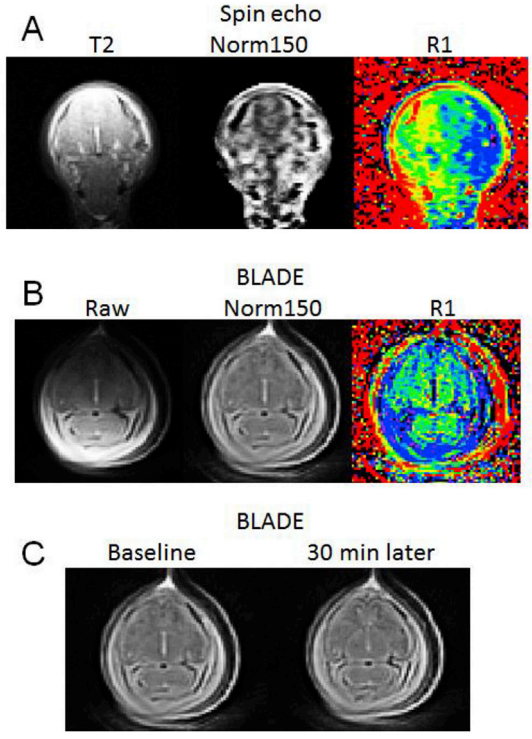

Fig. 3. Representative images showing A) benefits from the 3D printed clip and surface coil reception for collecting T2 weighted images but not for R1 images, B) benefits of BLADE acquisition and post-processing normalization to the TR 150 ms image (Norm150) to minimize B1 inhomogeneity's artifacts, coil and slice bias, and minimize motion artifacts resulting in improved anatomical images (Norm150) and R1 image quality, and C) reproducibility.

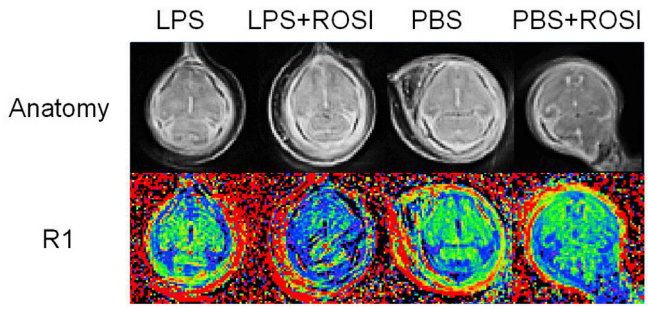

Fig. 4. *Top row*: Representative anatomical images (generated by normalizing to the TR 150 ms image) for each group studied in the LPS arm of the study. *Bottom row:* Corresponding R1 maps for each group studied herein.

3.3. Post-processing normalization to minimize coil and slice bias

Normalization to the shortest TR time visibly minimized B1 inhomogeneities (Fig. 3 B, compare "Raw" to "Norm150") and the expected bias of imperfect slice profiles on R1 [Chapter 18 in (Haacke et al., 1999)]. Combining the above procedures, sufficient R1 maps were collectable within and across groups (Figs. 3 C, Fig. 4, bottom row; Fig. 5).

3.4. QUEST MRI

Visual inspection of typical R1 images for the four groups (Fig. 4, bottom row) suggested that ROSI decreased R1 in the LPS group but not in the PBS group. Quantitative analysis of select brain ROI's (Fig. 5) found that the combined caudate-putamen and thalamus ROI R1 was reduced ($p = 0.0003$) with ROSI treatment in the LPS group, consistent with brain oxidative stress. On the other hand, ROSI did not decrease combined caudate-putamen and thalamus R1 in the PBS group ($p = 0.17$). Pons R1 was unaffected by ROSI regardless of LPS treatment ($p = 0.25$).

4. Discussion

In this study, we present a combination of two hardware and two software solutions that were sufficient for imaging fetal brains *in utero* without respiratory gating or the injection of a contrast agent. The present study addresses problems introduced by maternal and fetal motion (Hogers et al., 2000; Chapon et al., 2002; Ahrens et al., 2006; Deans et al., 2008; Wu and Zhang, 2016; Zhang et al., 2018). Some of the previous methodology used to address these problems involve respiratory gating but gating alone does not account for fetal motion (Hogers et al., 2000; Chapon et al., 2002; Ahrens et al., 2006; Deans et al., 2008; Neelavalli et al., 2014; Neelavalli et al., 2016; Wu and Zhang, 2016; Yadav et al., 2018). Also, some studies have injected contrast agents like manganese, but this approach has unclear clinical translation potential (Hogers et al., 2000; Chapon et al., 2002; Ahrens et al., 2006; Deans et al., 2008; Neelavalli et al., 2014; Neelavalli et al., 2016; Wu and Zhang, 2016; Yadav et al., 2018). In addition, fast imaging acquisitions, an approach with low spatial resolution, or a focus on the circulation are often used in imaging the fetal brain (Hogers et al., 2000; Chapon et al., 2002; Ahrens et al., 2006; Deans et al., 2008; Neelavalli et al., 2014; Neelavalli et al., 2016; Wu and Zhang, 2016; Yadav et al., 2018). Here, we used a combined approach that was sufficient for generating high enough spatial resolution images of fetal brain anatomy to measure neuronal oxidative stress linked with pre-term labor and delivery (Berrios-Otero et al., 2012;

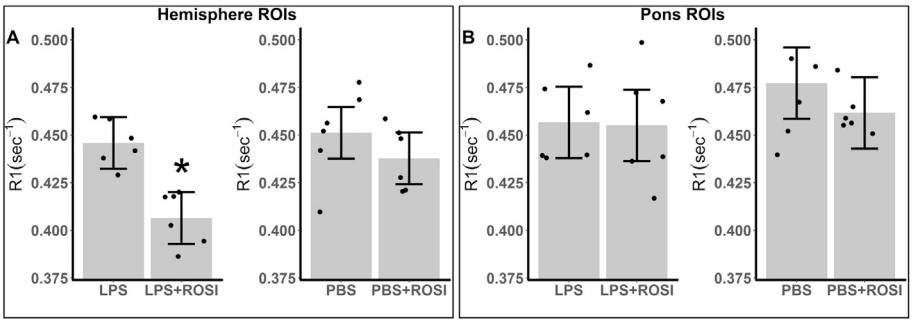

Fig. 5. Modeled mean A) hemisphere or B) Pons ROI R1's (illustrated in Fig. 2) from either LPS and LPS + ROSI groups *(left bargraph)* or PBS and PBS + ROSI *(right bargraph)*. All groups had n = 6 fetuses. Error bars: 95% confidence intervals. Asterisk = significant difference ($P < 0.05$).

Parasoglou et al., 2013).

Our approach found oxidative stress in the caudate-putamen and thalamus, but not in the pons region, in a mouse LPS model of intrauterine infection and preterm birth (Kannan et al., 2012; Chao et al., 2016). In humans, regional changes in cerebral blood flow have been observed in preterm infants following brain injury, but the significance of such local effects on brain oxidative stress is unclear (Mahdi et al., 2018). Another study reports changes in synaptic layers that appear region-specific following LPS injection in a sheep model (Strackx et al., 2015). Interpretation of the present regional differences awaits further experiments because few reports are available regarding regions of vulnerability for damage in the fetal brain *in utero*.

The use of isoflurane anesthesia during both the intra-amniotic injections and MRI experiments may be a potential confounder: in adult mice, isoflurane exposure can lead to increased cerebral blood and inhibition of complex I in addition to promoting neuroprotective preconditioning (Ludwig et al., 2004; Hirata et al., 2011; Bajwa, Lee et al., 2018). Pregnant rats exposed to high levels of isoflurane can have pups with decreased learning and memory and neurodegeneration (Wang et al., 2009; Palanisamy et al., 2011; Huang et al., 2018). However, it is unclear how isoflurane might influence the murine fetal brain *in utero* under the conditions of this study; further work is needed to address this concern.

This study has some limitations. Our combined approach currently examines only one fetus per dam to minimize the examination time and time under anesthesia. However, depending on the insult, examining a single fetus may not be a representative sample of the other fetuses. Also, by limiting the examination time, we likely did not have time to find the same slice orientation in each fetus, and this ultimately limited our choices for ROI that could be identified in each subject in the present study. To improve slice selection for more localized ROI analysis, future studies will investigate obtaining volumetric R1 measurements; obtaining precise multislice/3D spin-lattice measurements remains an area of active study by the field. Nonetheless, our combined approach was sufficient for generating high enough spatial resolution images of fetal brain anatomy to measure neuronal oxidative stress linked with pre-term labor and delivery.

Herein, we found evidence that treatment with ROSI can have anti-oxidative effects on the LPS-exposed fetal brain vs. the PBS-exposed brain demonstrating feasibility of QUEST MRI. The U.S. Food and Drug Administration (FDA) considers ROSI as a Category C drug and is not recommended for use during pregnancy (https://www.fda.gov/downloads/Drugs/DrugSafety/PostmarketDrugSafetyInformationforPatientsandProviders/UCM143413.pdf). On the other hand, preclinical studies did not find evidence of harm to the fetus following administration of ROSI during pregnancy (Klinkner et al., 2006; Kohan-Ghadr et al., 2018). Possible translational application of QUEST MRI to humans may involve, for example, an FDA-approved synthetic analog of progesterone, which was found to be a powerful neuroprotective anti-oxidant (Byrne et al., 2016). Future studies may investigate using vaginal progesterone to prevent fetal brain oxidative stress as measured by QUEST MRI (Hassan et al., 2011; Furcron et al., 2015; Conde-Agudelo and Romero, 2016; Romero et al., 2016; Romero et al., 2017; Conde-Agudelo et al., 2018; Romero et al., 2018)].

In summary, we found a combined approach that generated sufficient spatial resolution images of the fetal brain *in utero* to test a hypothesis about brain oxidative stress in a model of pre-term labor and delivery. Given that anti-oxidant treatment is not contraindicated in pregnancy, we anticipate future preclinical and clinical studies that combine QUEST MRI maps of oxidative stress, perhaps together with circulatory and functional MRI maps, to improve fetal health outcomes.

Acknowledgements

This research was supported, in part, by the Perinatology Research Branch, Division of Obstetrics and Maternal-Fetal Medicine, Division of Intramural Research, *Eunice Kennedy Shriver* National Institute of Child Health and Human Development, National Institutes of Health, U.S. Department of Health and Human Services (NICHD/NIH/DHHS); and, in part, with federal funds from NICHD/NIH/DHHS under Contract No. HHSN275201300006C. Dr. Romero has contributed to this work as part of his official duties as an employee of the United States Federal Government. NG-L was also supported by the Wayne State University Perinatal Initiative in Maternal, Perinatal and Child Health. This research was also supported by the National Eye Institute (RO1 EY026584, RO1 AG058171 to BAB). We thank Chengrui (Richard) Zou for facilitating the transport of the animals between animal facilities.

References

Ahrens, E.T., Srinivas, M., Capuano, S., Simhan, H.N., Schatten, G.P., 2006. Magnetic resonance imaging of embryonic and fetal development in model systems. Methods Mol. Med. 124, 87–101.

Bajwa, N.M., Lee, J.B., Halavi, S., Hartman, R.E., Obenaus, A., 2019. Repeated isoflurane in adult male mice leads to acute and persistent motor decrements with long-term modifications in corpus callosum microstructural integrity. J. Neurosci. Res. 97, 332–345.

Berkowitz, B.A., 2018. Oxidative stress measured in vivo without an exogenous contrast agent using QUEST MRI. J. Magn. Reson. 291, 94–100.

Berkowitz, B.A., Bredell, B.X., Davis, C., Samardzija, M., Grimm, C., Roberts, R., 2015. Measuring in vivo free radical production by the outer retina. Investig. Ophthalmol. Vis. Sci. 56 (13), 7931–7938.

Berkowitz, B.A., Lewin, A.S., Biswal, M.R., Bredell, B.X., Davis, C., Roberts, R., 2016. MRI of retinal free radical production with laminar resolution in vivo. Investig. Ophthalmol. Vis. Sci. 57 (2), 577–585.

Berrios-Otero, C.A., Nieman, B.J., Parasoglou, P., Turnbull, D.H., 2012. In utero phenotyping of mouse embryonic vasculature with MRI. Magn. Reson. Med. 67 (1), 251–257.

Byrne, A.M., Ruiz-Lopez, A.M., Roche, S.L., Moloney, J.N., Wyse-Jackson, A.C., Cotter, T.G., 2016. The synthetic progestin norgestrel modulates Nrf2 signaling and acts as an antioxidant in a model of retinal degeneration. Redox Biol. 10, 128–139.

Chao, M.W., Chen, C.P., Yang, Y.H., Chuang, Y.C., Chu, T.Y., Tseng, C.Y., 2016. N-acetylcysteine attenuates lipopolysaccharide-induced impairment in lamination of Ctip2-and Tbr1- expressing cortical neurons in the developing rat fetal brain. Sci. Rep. 6, 32373.

Chapon, C., Franconi, F., Roux, J., Marescaux, L., Le Jeune, J.J., Lemaire, L., 2002. In utero time-course assessment of mouse embryo development using high resolution magnetic resonance imaging. Anat. Embryol. 206 (1–2), 131–137.
Conde-Agudelo, A., Romero, R., 2016. Vaginal progesterone to prevent preterm birth in pregnant women with a sonographic short cervix: clinical and public health implications. Am. J. Obstet. Gynecol. 214 (2), 235–242.
Conde-Agudelo, A., Romero, R., Da Fonseca, E., O'Brien, J.M., Cetingoz, E., Creasy, G.W., Hassan, S.S., Erez, O., Pacora, P., Nicolaides, K.H., 2018. Vaginal progesterone is as effective as cervical cerclage to prevent preterm birth in women with a singleton gestation, previous spontaneous preterm birth, and a short cervix: updated indirect comparison meta-analysis. Am. J. Obstet. Gynecol. 219 (1), 10–25.
Deans, A.E., Wadghiri, Y.Z., Berrios-Otero, C.A., Turnbull, D.H., 2008. Mn enhancement and respiratory gating for in utero MRI of the embryonic mouse central nervous system. Magn. Reson. Med. 59 (6), 1320–1328.
Furcron, A.E., Romero, R., Plazyo, O., Unkel, R., Xu, Y., Hassan, S.S., Chaemsaithong, P., Mahajan, A., Gomez-Lopez, N., 2015. Vaginal progesterone, but not 17alpha-hydroxyprogesterone caproate, has antiinflammatory effects at the murine maternal-fetal interface. Am. J. Obstet. Gynecol. 213 (6), 846.e841-846.e819.
Ginsberg, Y., Khatib, N., Weiner, Z., Beloosesky, R., 2017. Maternal inflammation, fetal brain implications and suggested neuroprotection: a summary of 10 Years of research in animal models. Rambam Maimonides Med. J. 8 (2), e0028.
Gomez, R., Romero, R., Ghezzi, F., Yoon, B.H., Mazor, M., Berry, S.M., 1998. The fetal inflammatory response syndrom. Am. J. Obstet. Gynecol. 179 (1), 194–202.
Gomez-Lopez, N., Romero, R., Arenas-Hernandez, M., Panaitescu, B., Garcia-Flores, V., Mial, T.N., Sahi, A., Hassan, S.S., 2018. Intra-amniotic administration of lipopolysaccharide induces spontaneous preterm labor and birth in the absence of a body temperature change. J. Matern. Fetal Neonatal Med. 31 (4), 439–446.
Gomez-Lopez, N., Romero, R., Arenas-Hernandez, M., Schwenkel, G., St Louis, D., Hassan, S.S., Mial, T.N., 2017. In vivo activation of invariant natural killer T cells induces systemic and local alterations in T-cell subsets prior to preterm birth. Clin. Exp. Immunol. 189 (2), 211–225.
Gotsch, F., Romero, R., Kusanovic, J.P., Mazaki-Tovi, S., Pineles, B.L., Erez, O., Espinoza, J., Hassan, S.S., 2007. he fetal inflammatory response syndrome. Clin. Obstet. Gynecol. 50 (3), 652–683.
Haacke, E.M., Brown, R.W., Thompson, M.R., Venkatesan, R., 1999. Magnetic Resonance Imaging: Physical Principles and Sequence Design. Wiley.
Hassan, S.S., Romero, R., Vidyadhari, D., Fusey, S., Baxter, J.K., Khandelwal, M., Vijayaraghavan, J., Trivedi, Y., Soma-Pillay, P., Sambarey, P., Dayal, A., Potapov, V., O'Brien, J., Astakhov, V., Yuzko, O., Kinzler, W., Dattel, B., Sehdev, H., Mazheika, L., Manchulenko, D., Gervasi, M.T., Sullivan, L., Conde-Agudelo, A., Phillips, J.A., Creasy, G.W., 2011. Vaginal progesterone reduces the rate of preterm birth in women with a sonographic short cervix: a multicenter, randomized, double-blind, placebo-controlled trial. Ultrasound Obstet. Gynecol. 38 (1), 18–31.
Hirata, N., Shim, Y.H., Pravdic, D., Lohr, N.L., Pratt Jr., P.F., Weihrauch, D., Kersten, J.R., Warltier, D.C., Bosnjak, Z.J., Bienengraeber, M., 2011. Isoflurane differentially modulates mitochondrial reactive oxygen species production via forward versus reverse electron transport flow: implications for preconditioning. Anesthesiology 115 (3), 531–540.
Hogers, B., Gross, D., Lehmann, V., Zick, K., De Groot, H.J., Gittenberger-De Groot, A.C., Poelmann, R.E., 2000. Magnetic resonance microscopy of mouse embryos in utero. Anat. Rec. 260 (4), 373–377.
Huang, W., Dong, Y., Zhao, G., Wang, Y., Jiang, J., Zhao, P., 2018. Influence of isoflurane exposure in pregnant rats on the learning and memory of offsprings. BMC Anesthesiol. 18 (1), 5.
Kadam, L., Gomez-Lopez, N., Mial, T.N., Kohan-Ghadr, H.R., Drewlo, S., 2017. Rosiglitazone regulates TLR4 and rescues HO-1 and NRF2 expression in myometrial and decidual macrophages in inflammation-induced preterm birth. Reprod. Sci. 24 (12), 1590–1599.
Kannan, S., Dai, H., Navath, R.S., Balakrishnan, B., Jyoti, A., Janisse, J., Romero, R., Kannan, R.M., 2012. Dendrimer-based postnatal therapy for neuroinflammation and cerebral palsy in a rabbit model. Sci. Transl. Med. 4 (130), 130ra146-130ra146.
Klinkner, D.B., Lim, H.J., Strawn Jr., E.Y., Oldham, K.T., Sander, T.L., 2006. An in vivo murine model of rosiglitazone use in pregnancy. Fertil. Steril. 86 (4 Suppl. l), 1074–1079.
Kohan-Ghadr, H.R., Kilburn, B.A., Kadam, L., Johnson, E., Kolb, B.L., Rodriguez-Kovacs, J., Hertz, M., Armant, D.R., Drewlo, S., 2018. Rosiglitazone augments antioxidant response in the human trophoblast and prevents apoptosis. Biol. Reprod. https://doi.org/10.1093/biolre/ioy186.
Ludwig, L.M., Tanaka, K., Eells, J.T., Weihrauch, D., Pagel, P.S., Kersten, J.R., Warltier, D.C., 2004. Preconditioning by isoflurane is mediated by reactive oxygen species generated from mitochondrial electron transport chain complex III. Anesth. Analg. 99 (5), 1308–1315.
Mahdi, E.S., Bouyssi-Kobar, M., Jacobs, M.B., Murnick, J., Chang, T., Limperopoulos, C., 2018. Cerebral perfusion is perturbed by preterm birth and brain injury. AJNR. Am. J. Neuroradiol. 39 (7), 1330–1335.
Neelavalli, J., Krishnamurthy, U., Jella, P.K., Mody, S.S., Yadav, B.K., Hendershot, K., Hernandez-Andrade, E., Yeo, L., Cabrera, M.D., Haacke, E.M., Hassan, S.S., Romero, R., 2016. Magnetic resonance angiography of fetal vasculature at 3.0 T. Eur. Radiol. 26 (12), 4570–4576.
Neelavalli, J., Mody, S., Yeo, L., Jella, P.K., Korzeniewski, S.J., Saleem, S., Katkuri, Y., Bahado-Singh, R.O., Hassan, S.S., Haacke, E.M., Romero, R., Thomason, M.E., 2014. MR venography of the fetal brain using susceptibility weighted imaging. J. Magn. Reson. Imag. 40 (4), 949–957.
Palanisamy, A., Baxter, M.G., Keel, P.K., Xie, Z., Crosby, G., Culley, D.J., 2011. Rats exposed to isoflurane in utero during early gestation are behaviorally abnormal as adults. Anesthesiology 114 (3), 521–528.
Parasoglou, P., Berrios-Otero, C.A., Nieman, B.J., Turnbull, D.H., 2013. High-resolution MRI of early-stage mouse embryos. NMR Biomed. 26 (2), 224–231.
Petiet, A.E., Kaufman, M.H., Goddeeris, M.M., Brandenburg, J., Elmore, S.A., Johnson, G.A., 2008. High-resolution magnetic resonance histology of the embryonic and neonatal mouse: a 4D atlas and morphologic database. Proc. Natl. Acad. Sci. U. S. A. 105 (34), 12331–12336.
Pipe, J.G., 1999. Motion correction with PROPELLER MRI: application to head motion and free-breathing cardiac imaging. Magn. Reson. Med. 42 (5), 963–969.
Romero, R., Conde-Agudelo, A., Da Fonseca, E., O'Brien, J.M., Cetingoz, E., Creasy, G.W., Hassan, S.S., Nicolaides, K.H., 2018. Vaginal progesterone for preventing preterm birth and adverse perinatal outcomes in singleton gestations with a short cervix: a meta-analysis of individual patient data. Am. J. Obstet. Gynecol. 218 (2), 161–180.
Romero, R., Conde-Agudelo, A., El-Refaie, W., Rode, L., Brizot, M.L., Cetingoz, E., Serra, V., Da Fonseca, E., Abdelhafez, M.S., Tabor, A., Perales, A., Hassan, S.S., Nicolaides, K.H., 2017. Vaginal progesterone decreases preterm birth and neonatal morbidity and mortality in women with a twin gestation and a short cervix: an updated meta-analysis of individual patient data. Ultrasound Obstet. Gynecol. 49 (3), 303–314.
Romero, R., Dey, S.K., Fisher, S.J., 2014. Preterm labor: one syndrome, many causes. Science 345 (6198), 760–765.
Romero, R., Nicolaides, K.H., Conde-Agudelo, A., O'Brien, J.M., Cetingoz, E., Da Fonseca, E., Creasy, G.W., Hassan, S.S., 2016. Vaginal progesterone decreases preterm birth </= 34 weeks of gestation in women with a singleton pregnancy and a short cervix: an updated meta-analysis including data from the OPPTIMUM study. Ultrasound Obstet. Gynecol. 48 (3), 308–317.
St Louis, D., Romero, R., Plazyo, O., Arenas-Hernandez, M., Panaitescu, B., Xu, Y., Milovic, T., Xu, Z., Bhatti, G., Mi, Q.S., Drewlo, S., Tarca, A.L., Hassan, S.S., Gomez-Lopez, N., 2016. Invariant NKT cell activation induces late preterm birth that is attenuated by rosiglitazone. J. Immunol. 196 (3), 1044–1059.
Strackx, E., Jellema, R.K., Rieke, R., Gussenhoven, R., Vles, J.S., Kramer, B.W., Gavilanes, A.W., 2015. Intra-amniotic LPS induced region-specific changes in presynaptic bouton densities in the ovine fetal brain. BioMed Res. Int. 2015, 276029.
Wang, S., Peretich, K., Zhao, Y., Liang, G., Meng, Q., Wei, H., 2009. Anesthesia-induced neurodegeneration in fetal rat brains. Pediatr. Res. 66 (4), 435–440.
Wu, D., Zhang, J., 2016. Recent progress in magnetic resonance imaging of the embryonic and neonatal mouse brain. Front. Neuroanat. 10, 18.
Xu, Y., Romero, R., Miller, D., Kadam, L., Mial, T.N., Plazyo, O., Garcia-Flores, V., Hassan, S.S., Xu, Z., Tarca, A.L., Drewlo, S., Gomez-Lopez, N., 2016. An M1-like macrophage polarization in decidual tissue during spontaneous preterm labor that is attenuated by rosiglitazone treatment. J. Immunol. 196 (6), 2476–2491.
Yadav, B.K., Krishnamurthy, U., Buch, S., Jella, P., Hernandez-Andrade, E., Yeo, L., Korzeniewski, S.J., Trifan, A., Hassan, S.S., Haacke, E.M., Romero, R., Neelavalli, J., 2018. Imaging putative foetal cerebral blood oxygenation using susceptibility weighted imaging (SWI). Eur. Radiol. 28 (5), 1884–1890.
Zhang, J., Wu, D., Turnbull, D.H., 2018. In utero MRI of mouse embryos. Methods Mol. Biol. 1718, 285–296.